A Machine Learning-Enabled Process Optimization of Ultra-Fast Flow Chemistry with Multiple Reaction Metrics

Dogancan Karan,[a] Guoying Chen,[a] Nicholas Jose,[a,b,c], Jiaru Bai[b], Paul McDaid[d] and Alexei A. Lapkin*[a,b,e]

[a]Cambridge Centre for Advanced Research and Education in Singapore, CARES Ltd. 1 CREATE Way, CREATE Tower #05-05, Singapore 138602, Singapore

[b]Department of Chemical Engineering and Biotechnology, University of Cambridge, Cambridge CB3 0AS, UK

[c]Accelerated Materials Ltd, 71-75, Shelton Street, WC2H 9JK London, UK

[d]Pfizer Private Limited, Global Technology & Engineering, PGS, Loughbeg, Ringaskiddy, Co. Cork, Ireland

[e]Innovation Centre in Digital Molecular Technologies, Yusuf Hamied Department of Chemistry, University of Cambridge, Lensfield Rd, Cambridge CB2 1EW, UK

Electronic Supporting Information (ESI)

Table of Contents

1. Images of the Experimental Setup

Figure S1 Photograph of the experimental setup

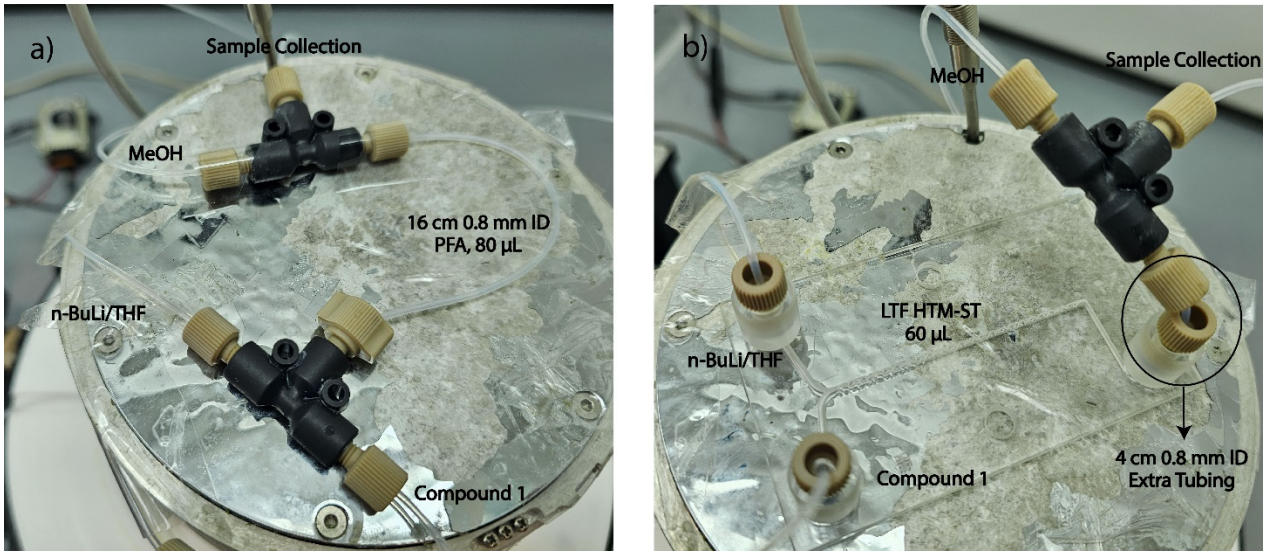

Figure S2 Photographs of the two different reactors used in this work.

2. Analytical Protocol

The analysis of samples at the end of the reaction was performed by using Agilent 1260 Infinity II UPLC-MS equipped with Agilent ZORBAX SB-C18 1.8 µm, 2.1 x 50 mm column. Compounds were resolved using the following protocol: The initial mobile phase mixture was 5:95 (v/v) binary mixture of acetonitrile and water (with 0.05 % Trifluoroacetic acid by volume) flowing at 0.4 mL/min. Immediately after the sample injection, the flow rate of acetonitrile/water mixture was changed to 0.7 mL/min. Thereafter, the flow rate ratio of the mixture was steadily changed to 95:5 over 4.5 minutes. Next, the flow rate ratio of the mixture was returned to 5:95 over a duration of 3 minutes. Finally, the flow rate ratio was held constant for 0.5 minutes after which the analysis was complete, and the method returned to flow rate of 0.4 mL/min until the next sample was introduced. The total analysis time for one sample was 8 minutes. A single wavelength of 254 nm was used throughout the analysis and injection volume was 0.4 µL.

The reaction yield and the impurity amount were determined from the HPLC chromatograms through area normalization. We tested the response factor of all the components in the reactor effluent and found that they all have similar response to UV light. Consequently, area normalization could be used to calculate the yield and impurity. An example HPLC result is shown in **Figure S3**.

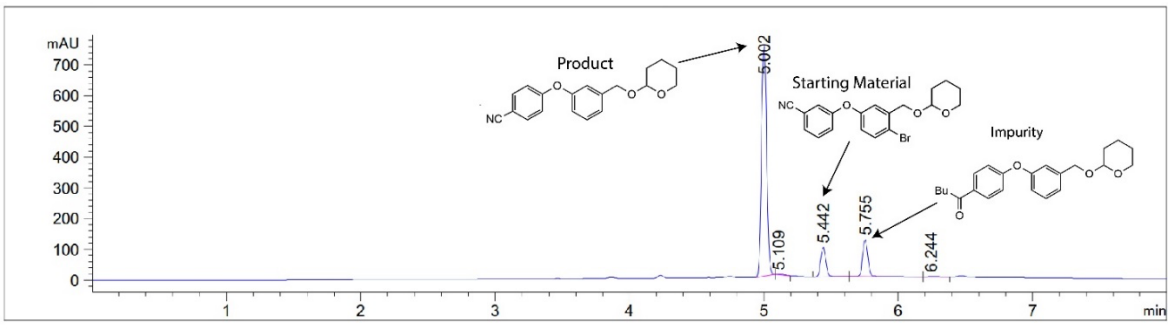

Figure S3. An example HPLC result of Br-Li exchange reaction.

3. Event Sequence

Below, a simple event sequence is provided for a single data point collection and processing:

Flab

- Set the Polar Bear temperature at T.
- Purge cooling loops (t = 30 s, Q = 0.5 mL/min)
- Set pump flow rates THF = Q_{THF}, n-BuLi = $Q_{n\text{-}BuLi}$, **1** = 1 mL/min
- Wait for $t_{I.}$
- Set Pump flow rates **1** = Q_1, MeOH = Q_{MeOH} mL/min.
- Wait for $t_{II.}$
- Collect sample (off-line)
- Set pump flow rates MeOH = 0, n-BuLi= 0, THF = 1, **1** = 1 mL/min.
- Wait for $t_{III.}$
- Set pump flow rates THF = 0, **1** = 0 mL/min.

Offline

- Analyze the sample.
- Manually key the result in log file.

Summit

- Populate the data.
- Suggest the next condition via TSEMO.
- Calculate the time scales and flow rates.

Detailed description of the calculation of t_I - t_{III} and pump flow rates are provided below.

4. Flow Rate Calculation

The calculation of the flow rates of individual streams ($Q_{\mathbf{1}}$, Q_{THF}, nQ_{n-BuLi} and Q_{MeOH}) started with calculating the total flow rate of **1**, THF, n-BuLi (Q_T) from the experimental condition suggested by TSEMO or LHS.

$$Q_T = \frac{V_R}{\tau} \tag{S1}$$

where, V_R is the volume of the reactor (T-mixer with capillary tube or microchip reactor), τ is the residence time. We fixed the concentration of the n-BuLi as 0.35 M after it was diluted with THF throughout the study. Therefore, the flow rates of the individual streams were calculated from the following equations by using mass balance:

$$Q_{\mathbf{1}} = \frac{Q_T}{1 + \frac{C_{\mathbf{1}} \times (nBuLi\ Eq)}{0.35}} \tag{S2}$$

$$Q_{n-BuLi} = \frac{0.35\ \times (Q_T - Q_{\mathbf{1}})}{C_{n-BuLi,stock}} \tag{S3}$$

$$Q_{THF} = Q_T - Q_{\mathbf{1}} - Q_{n-BuLi} \tag{S4}$$

where, $C_{\mathbf{1}}$ is the concentration of aryl bromide **1** in the stock solution, $nBuLi\ Eq$ is the molar equivalence of n-BuLi suggested by TSEMO or LHS, $C_{n-BuLi,stock}$ is the concentration of n-BuLi in the stock solution (2 M). Methanol flow rate (Q_{MeOH}) was equal to Q_T up to Q_T = 16 mL/min. For the cases where Q_T > 16 mL/min, methanol flow rate was always 16 mL/min.

5. Analysis of Dispersion Characteristics and Prediction of Steady State Time

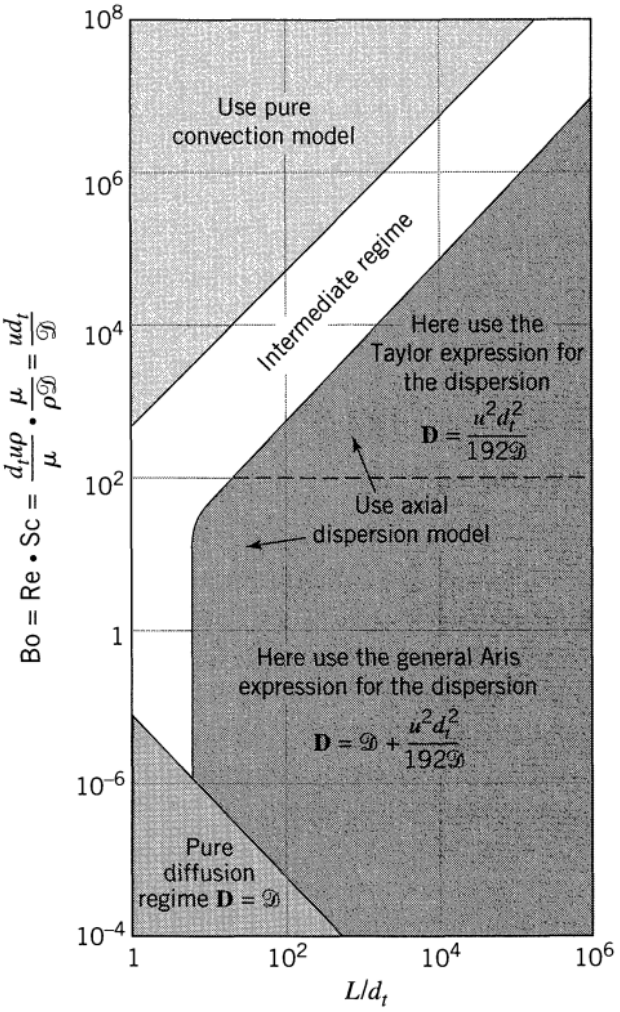

Figure S4. Flow map used to identify the dispersion regime in this work[1]

The event sequence to collect a datapoint described in the previous section resulted in dispersion in our system due to laminar flow regime. Dispersion occurs in our system i) within n-BuLi cooling loop when n-BuLi/THF mixture is replaced by washing THF, ii) within the reaction zone, iii) withing the sample collection zone. We used the map shown in **Figure S4** to identify the dispersion regime in our system. We used the upper and lower limits of the residence time and sociometric ratios in **Scheme 1c** to calculate the upper and lower limits of the Bodenstein number in our system. Our calculations revealed that the majority of the decision space could be modelled by axial dispersion model.

Dispersion within n-BuLi cooling loop was calculated as the summation of the mean residence times in the static mixer unit and the cooling line. Due to good radial mixing within the static mixer, the mean residence time equals plug flow residence time:

$$t_{mixer} = \frac{V_{mixer}}{Q_{n-BuLi} + Q_{THF}} \quad \text{(S5)}$$

where, V_{mixer} is the volume of the static mixer (0.6 mL). The mean residence time in the cooling line due to dispersion was estimated from **Equation S6**:

$$t_{n-BuLi} = \frac{V_{n-BuLi}}{Q_{n-BuLi} + Q_{THF}}\left(1 + \frac{2}{Pe_{n-BuLi}}\right) \quad \text{(S6)}$$

where, V_{n-BuLi} is the volume of the n-BuLi cooling line, Pe_{n-BuLi} is the reactor Peclet number in n-BuLi cooling loop. The reactor Peclet number was:

$$Pe_{n-BuLi} = \frac{U_{n-BuLi/THF} \times L_{n-BuLi}}{\boldsymbol{D}_{n-BuLi}} \quad \text{(S7)}$$

where, $U_{n-BuLi/THF}$ is the superficial velocity of n-BuLi/THF mixture in n-BuLi cooling loop (m/s), L_{n-BuLi} is the length of the n-BuLi cooling loop (m), $\boldsymbol{D}_{n-BuLi}$ is the axial dispersion coefficient of n-BuLi in n-BuLi cooling loop. The axial dispersion coefficient was calculated from:

$$\boldsymbol{D}_{n-BuLi} = \frac{{U_{n-BuLi/THF}}^2 d_t^2}{192 D_{n-BuLi}} \quad \text{(S8)}$$

d_t is the tube diameter (m), D_{n-BuLi} is the molecular diffusivity of n-BuLi in THF. Since the volumetric flow rate of n-BuLi was at least one order of magnitude lower than that of THF under different experimental conditions, we assumed that n-BuLi is dissolved purely in THF,

and we did not take the presence of cyclohexane into account when we calculated the molecular diffusivity. The molecular diffusivity of n-BuLi in THF was estimated from Wilkie-Chang Equation:

$$D_{n-BuLi}(m^2/s) = 7.4 \times 10^{-12} \frac{\sqrt{\psi_{THF} MW_{THF}}T}{\eta_{THF} \bar{V}_{n-BuLi}} \quad \text{(S9)}$$

ψ_{THF} is the association factor of THF (ψ_{THF} = 1), MW_{THF} is the molecular weight of THF, (g/mol), T is the reaction temperature (K), η_{THF} is the viscosity of THF (cP), and $\bar{V}_{n-BuLi}$ is the molar volume of n-BuLi at its boiling point (mL/mol). $\bar{V}_{n-BuLi}$ was predicted as 422.4 mL/mol from group contribution method[2]. Furthermore, since the viscosity is a temperature-dependent property, the viscosity of THF at different reaction temperatures was predicted by applying linear regression on the data shown in **Figure S5.**

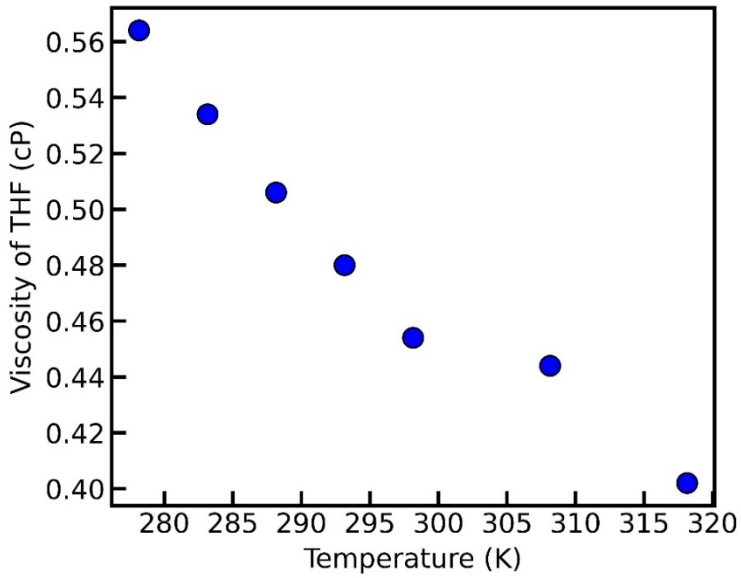

Figure S5. Dynamic viscosity data of THF at different temperatures [3].

As a result, the mean residence time in n-BuLi cooling loop was estimated as:

$$t_{m,n-BuLi} = t_{mixer} + t_{n-BuLi} \quad \text{(S10)}$$

Since the time scale in the reaction zone (0.185 – 1.2 s) is significantly lower than the time scales in the cooling loops, we assumed that the dispersion in the reaction zone does not have any influence on the overall steady state time of the system.

The dispersion in the sample collection zone was estimated from **Equation S11**.

$$t_{Sample\ Collection} = \frac{V_{Sample\ Collection}}{Q_T + Q_{MeOH}}\left(1 + \frac{2}{Pe_1}\right) \quad \text{(S11)}$$

where, $V_{Sample\ Collection}$ is the volume of the sample collection line, Pe_3 is the reactor Peclet number of **3** in the sample collection line. Even if the reaction forms the mixture of **1/2/3 (Scheme 1b)** which have different diffusivities, we assumed that the product stream only contains **3** to simply the calculations. Similar to described above, **Equations S7-9** were used to calculate the necessary valuables. 648.78 mL/mol was used as molar volume of **3** at its boiling point from group contribution method.

Finally, since the cooling loop of **1** was always filled with the solution of **1**, and no THF washing was applied, the mean residence time of **1** in the cooling (t_1) loop could be calculated from the plug flow residence time.

$$t_1 = \frac{V_1}{Q_1} \times 60 \quad \text{(S11)}$$

Similar calculations were made to estimate the time required to remove all the unreacted n-BuLi and **1/2/3** remained in the system during THF washing by using the appropriate values in **Equations S5-10.** Finally, time scales in the event sequence described above were calculated as follows: $t_I = t_{m,n-BuLi} - t_1$, $t_{II} = t_{m,n-BuLi} + t_{Sample\ Collection}$, and washing time t_{III} was calculated in the same way as t_{II} with modified flow rates. This workflow was applied on 15 randomly generated experimental conditions to highlight the difference in steady state times (t_{II}) when plug flow model and our dispersion model were used. The results in **Figure S6** highlight that plug flow model underestimates the steady state time by 50 – 100 %. A sample collected under plug flow assumption would not belong to the real steady state of the system, and hence the results would be erroneous.

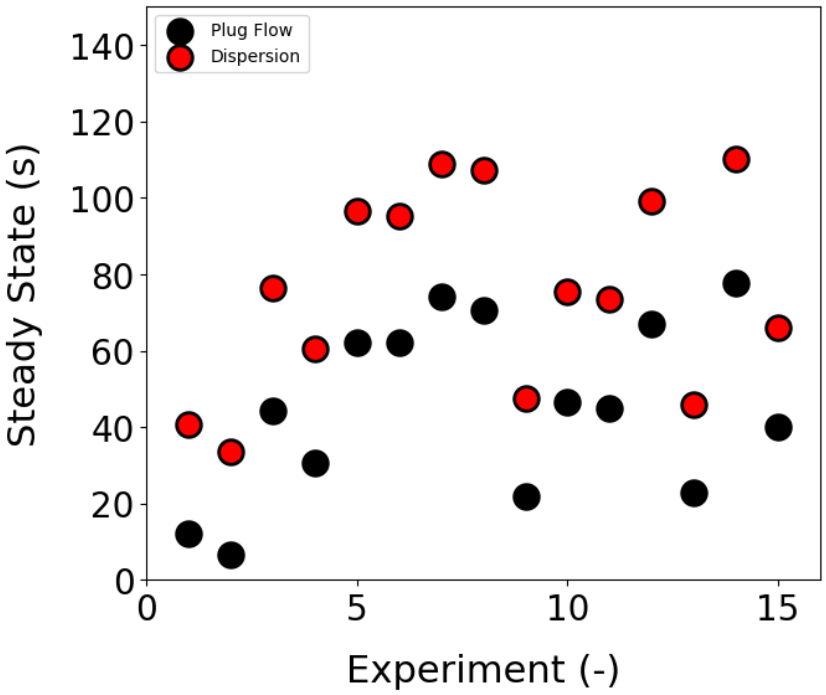

Figure S6 Prediction of the steady state times of 15 randomly generated samples by plug flow model and our dispersion model which highlight the significant difference between two approaches in steady state time prediction.

6. Preliminary Experiments of Br-Li Exchange Reaction

Summary of the preliminary experiments carried out to explore the upper limits of the continuous variables in the decision space are summarized in **Table S1** below. All the experiments in Table S1 were performed by using the T-mixer capillary tube reactor.

Table S1. A summary of the preliminary experiment to explore the boundaries of the decision space.

τ (s)	T (°C)	nBuLi	Yield (%)	Imp (%)	Observation
3	-10	0.95	2.4	5	Rector clogging
1.7	3	1.5	3	4.79	Reactor clogging
0.06	-26	1.33	0	0	Pump failure due to high flow rate
0.09	-26	1.33	0	0	Pump failure due to high flow rate
0.127	-28	1.24	0	0	Pump failure due to high flow rate
0.145	-28.6	1.24	0	0	Pump failure due to high flow rate
0.25	-20	0.85	59.6	4.4	C = 0.3 M, clogging due to high concentration of intermediate
0.25	-30	1.2	83	11.4	C = 0.2 M, clogging due to high concentration of intermediate
0.208	-7.3	0.87	46.75	0.48	C = 0.15 M, clogging due to high concentration of intermediate
0.841	-15.33	1.47	71.08	15	C = 0.15 M, clogging due to high concentration of intermediate

7. Optimization Data

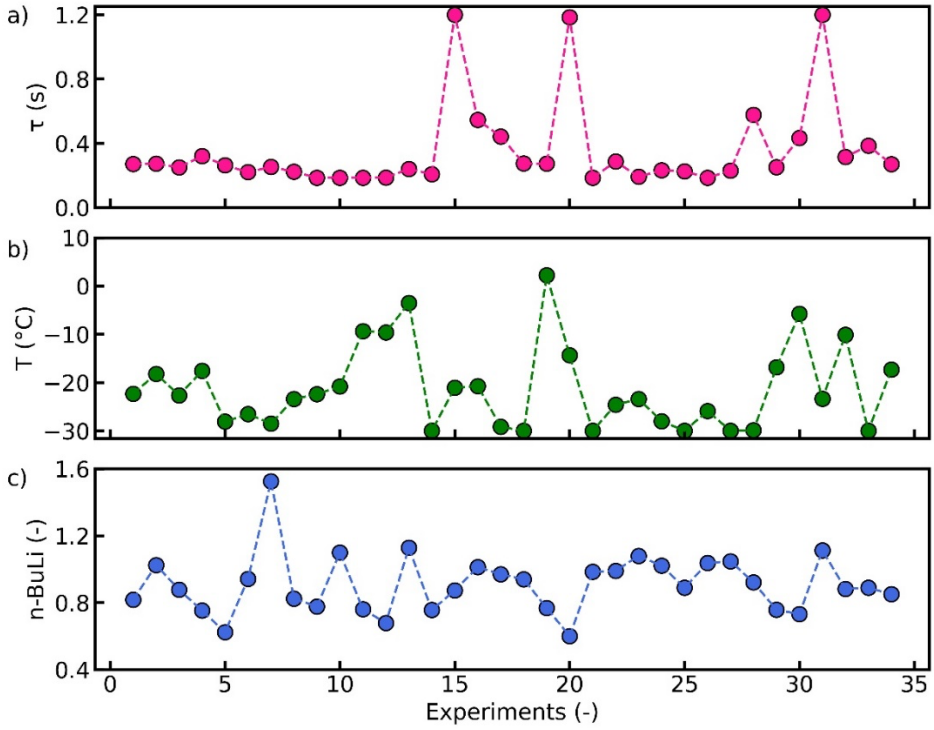

Figure S7. Variations in continuous variables during the course of optimization in three-parameter multi-objective optimization of Br-Li exchange reaction shown in **Figure 2** (12 training experiments with T-mixer capillary reactor).

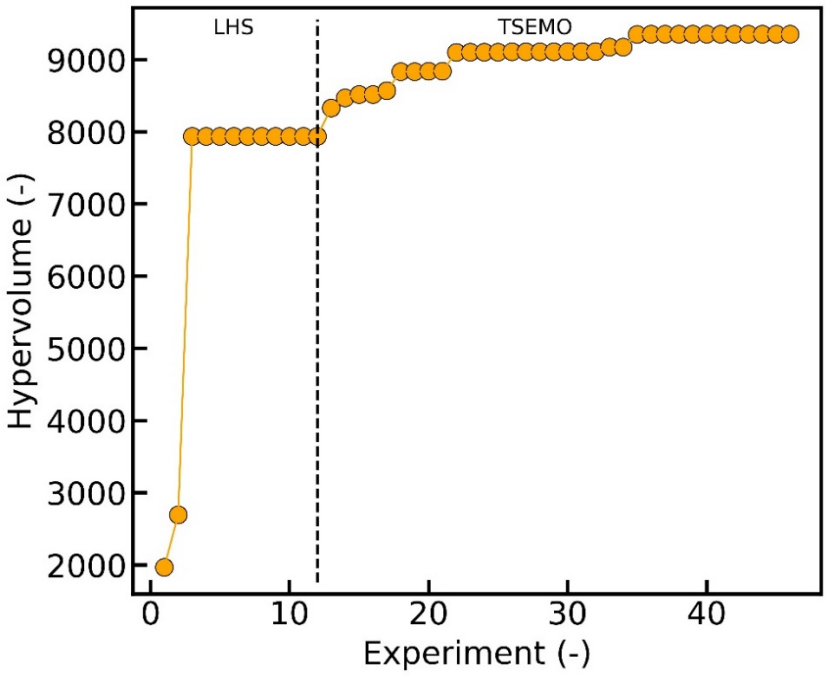

Figure S8. The change in the hypervolume during the course of optimization shown in **Figure 2.**

Table S2. Reaction conditions, yield, impurity and hypervolume values of optimization shown in **Figure 2.**

Experiment	τ (s)	T (°C)	nBuLi	Yield (%)	Impurity (%)	Hypervolume
Training-1	0.819	-28.33	0.642	21.29	7.63	1966.56
Training-2	1.073	-25.00	1.392	31.86	31.24	2693.35
Training-3	0.312	-21.67	1.058	85.089	6.74	7935.40
Training-4	0.396	-18.33	0.892	65.59	9.12	7935.40
Training-5	0.989	-15.00	0.975	24.03	13.44	7935.40
Training-6	0.65	-11.67	1.142	40.49	21.41	7935.40
Training-7	0.227	-8.33	1.558	56.9	40.48	7935.40
Training-8	0.481	-5.00	1.475	30.19	43.52	7935.40
Training-9	0.904	-1.67	0.808	29.47	13.3	7935.40
Training-10	0.735	1.67	1.225	31.55	43.79	7935.40
Training-11	0.566	5.00	1.308	53.55	28.14	7935.40
Training-12	0.481	8.33	0.808	49.99	9.75	7935.40
Optimization-1	0.271	-22.33	0.817	70.24	1.148	8328.18
Optimization-2	0.273	-18.21	1.024	86.62	7.4	8469.95
Optimization-3	0.25	-22.67	0.877	79.13	1.598	8515.67
Optimization-4	0.32	-17.60	0.753	63.45	1.152	8515.67
Optimization-5	0.263	-28.11	0.623	59.14	0.247	8568.95
Optimization-6	0.22	-26.53	0.942	89.11	3.69	8832.62
Optimization-7	0.253	-28.49	1.524	49.23	51.2	8832.62
Optimization-8	0.223	-23.43	0.824	80.41	1.218	8839.16
Optimization-9	0.185	-22.40	0.777	76.33	1.492	8839.16
Optimization-10	0.185	-20.82	1.099	91.95	8.149	9100.02
Optimization-11	0.185	-9.38	0.761	73.45	1.056	9101.56
Optimization-12	0.186	-9.63	0.678	61.1	1.81	9101.56
Optimization-13	0.24	-3.54	1.128	79.22	18.81	9101.56
Optimization-14	0.207	-30.00	0.756	73.68	0.728	9106.36
Optimization-15	1.2	-21.08	0.873	42.4	10.86	9106.36
Optimization-16	0.545	-20.74	1.012	71.88	8.6	9106.36
Optimization-17	0.442	-29.18	0.97	75.6	6.33	9106.36
Optimization-18	0.274	-30.00	0.939	88.58	3.16	9110.69
Optimization-19	0.273	2.21	0.768	61	1.58	9110.69
Optimization-20	1.184	-14.37	0.6	20.38	7.75	9110.69
Optimization-21	0.185	-30.00	0.984	92.25	1.74	9171.01
Optimization-22	0.286	-24.62	0.99	88.31	4.46	9171.01
Optimization-23	0.191	-23.42	1.079	94.11	4.129	9349.33
Optimization-24	0.232	-28.02	1.021	92.71	1.808	9350.40
Optimization-25	0.225	-30.00	0.889	87.2	2.35	9350.40
Optimization-26	0.185	-25.92	1.037	93.16	2.496	9350.40
Optimization-27	0.23	-30.00	1.047	93.328	3.385	9350.40
Optimization-28	0.577	-29.89	0.921	50.9	10	9350.40
Optimization-29	0.251	-16.84	0.757	63.58	1.251	9350.40
Optimization-30	0.433	-5.76	0.732	42.8	6.113	9350.40
Optimization-31	1.2	-23.38	1.112	29.69	20.28	9350.40
Optimization-32	0.314	-10.13	0.882	62.65	15.21	9350.40
Optimization-33	0.385	-30.00	0.889	67.96	6.783	9350.40
Optimization-34	0.269	-17.32	0.85	77.9	3.13	9350.40

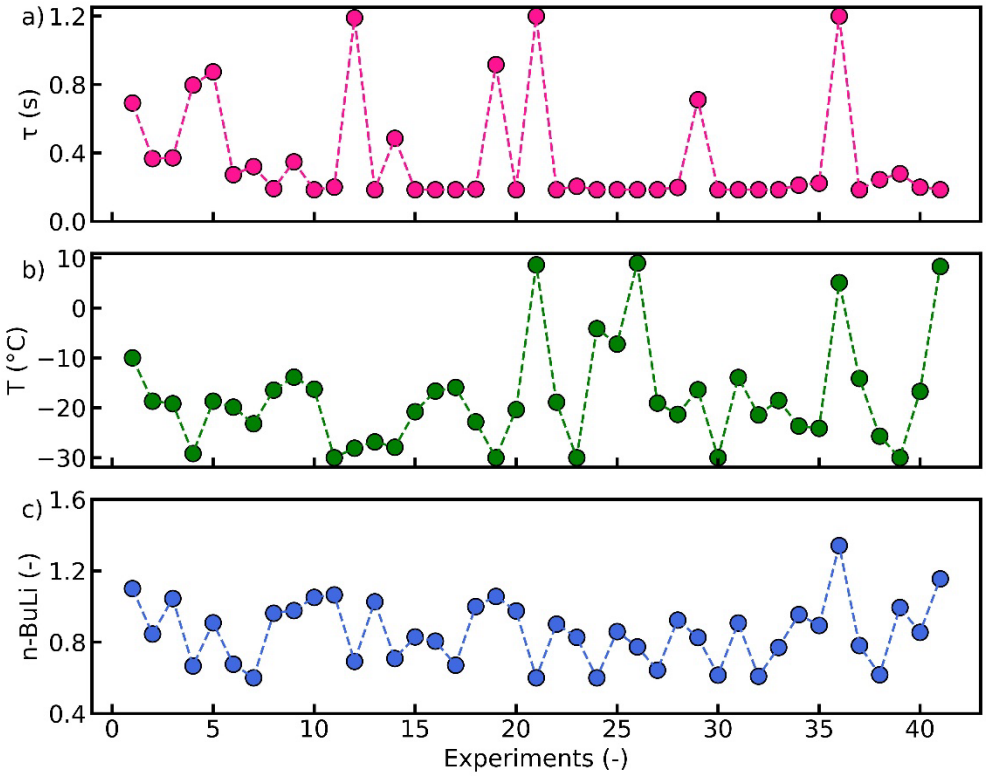

Figure S9. Variation in continuous variables during the course of optimization in three-parameter multi-objective optimization of Br-Li exchange reaction shown in **Figure 3** (3 training experiments with T-mixer capillary reactor).

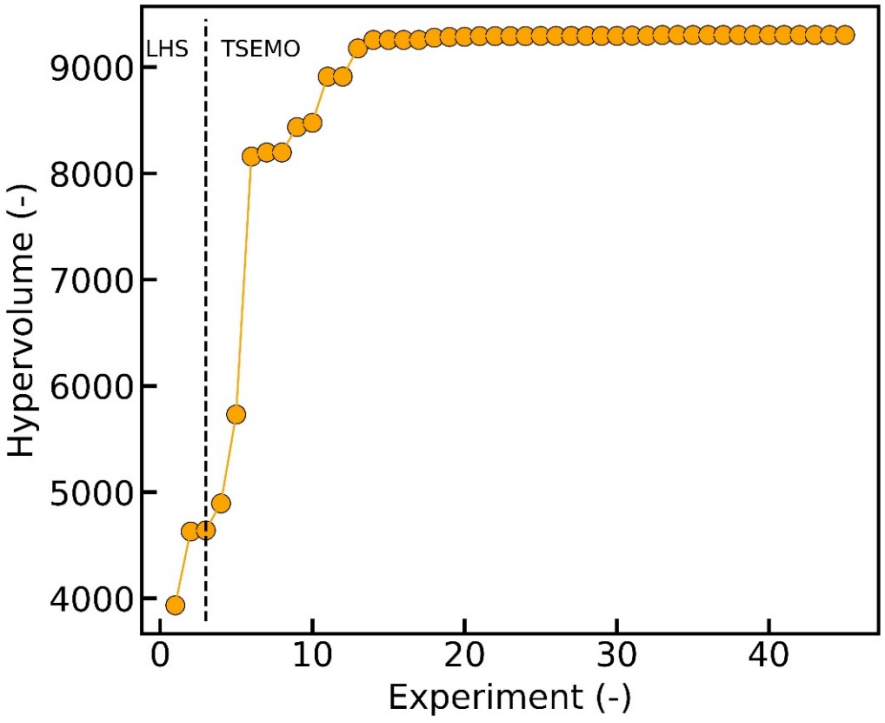

Figure S10. The change in the hypervolume during the course of optimization shown in **Figure 3.**

Table S3. Reaction conditions, yield, impurity and hypervolume values of optimization shown in **Figure 3.**

Experiment	τ (s)	T (°C)	nBuLi	Yield	Impurity	Hypervolume
Training-1	0.354	-23.33	1.433	60.42	34.88	3934.55
Training-2	1.031	-10.00	0.767	28.18	10.2	4630.03
Training-3	0.692	3.33	1.1	29.33	25.83	4640.44
Optimization-1	0.692	-10.00	1.1	44.52	18.74	4893.76
Optimization-2	0.367	-18.71	0.845	61.055	6.12	5731.84
Optimization-3	0.371	-19.17	1.045	88	9.9	8159.59
Optimization-4	0.797	-29.19	0.666	37.2	5.1	8197.53
Optimization-5	0.874	-18.70	0.908	24.88	14.12	8197.53
Optimization-6	0.273	-19.87	0.676	57.5	1.31	8436.16
Optimization-7	0.32	-23.21	0.6	54.41	0.56	8476.97
Optimization-8	0.192	-16.47	0.962	90.174	2.21	8910.67
Optimization-9	0.348	-13.85	0.977	70	10	8910.67
Optimization-10	0.185	-16.27	1.051	93	5.48	9177.79
Optimization-11	0.2	-30.00	1.065	93.8	4.8	9255.87
Optimization-12	1.19	-28.10	0.692	26.11	4.28	9255.87
Optimization-13	0.185	-26.83	1.026	91	4.39	9256.21
Optimization-14	0.485	-27.90	0.708	42.62	9	9256.21
Optimization-15	0.185	-20.77	0.829	81.1	1.31	9277.45
Optimization-16	0.185	-16.67	0.806	79.41	1	9285.20
Optimization-17	0.185	-15.91	0.671	64.32	0.97	9285.49
Optimization-18	0.188	-22.81	1	91.9	1.9	9292.97
Optimization-19	0.916	-30.00	1.056	30	22	9292.97
Optimization-20	0.185	-20.38	0.975	89.4	2.5	9292.97
Optimization-21	1.2	8.63	0.6	7.62	9.76	9292.97
Optimization-22	0.185	-18.89	0.901	85.5	1.6	9294.29
Optimization-23	0.205	-30.00	0.827	75.6	1.26	9294.29
Optimization-24	0.185	-4.13	0.6	56.25	0.76	9294.68
Optimization-25	0.185	-7.26	0.859	80	2.15	9294.68
Optimization-26	0.185	8.97	0.773	68	3.33	9294.68
Optimization-27	0.185	-19.06	0.643	62.5	0.81	9295.68
Optimization-28	0.198	-21.32	0.923	90.5	1.65	9296.93
Optimization-29	0.711	-16.39	0.826	28.17	15	9296.93
Optimization-30	0.185	-29.99	0.615	59.77	0.476	9303.20
Optimization-31	0.185	-13.94	0.907	86.57	1.65	9303.20
Optimization-32	0.185	-21.43	0.608	59	0.55	9303.20
Optimization-33	0.185	-18.52	0.77	75	1.84	9303.20
Optimization-34	0.212	-23.67	0.955	90	2.4	9303.20
Optimization-35	0.223	-24.11	0.893	89	2.7	9303.20
Optimization-36	1.2	5.07	1.341	30	43	9303.20
Optimization-37	0.185	-14.12	0.781	76	1.3	9303.20
Optimization-38	0.244	-25.70	0.617	60	0.705	9303.20
Optimization-39	0.279	-30.00	0.994	92	6	9303.20
Optimization-40	0.199	-16.72	0.855	74.3	4.124	9303.20
Optimization-41	0.185	8.31	1.155	81	13	9303.20

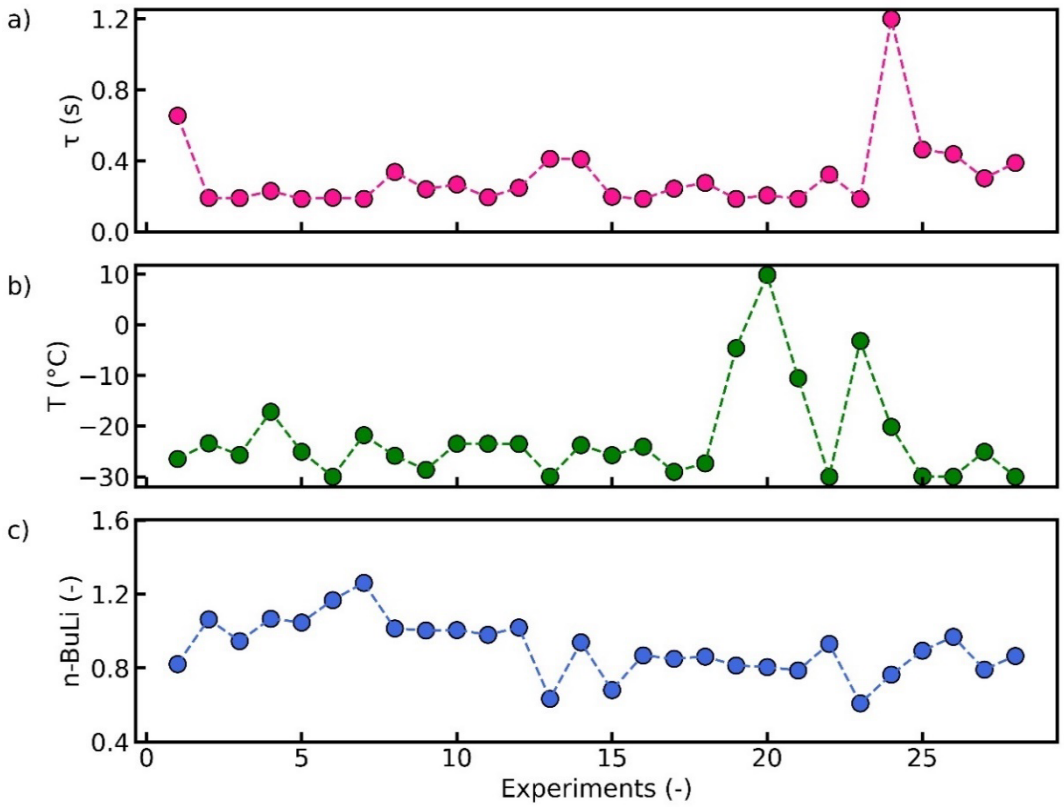

Figure S11. Variation in continuous variables during the course of optimization in three-parameter multi-objective optimization of Br-Li exchange reaction shown in **Figure 4** (12 training experiments with microchip reactor).

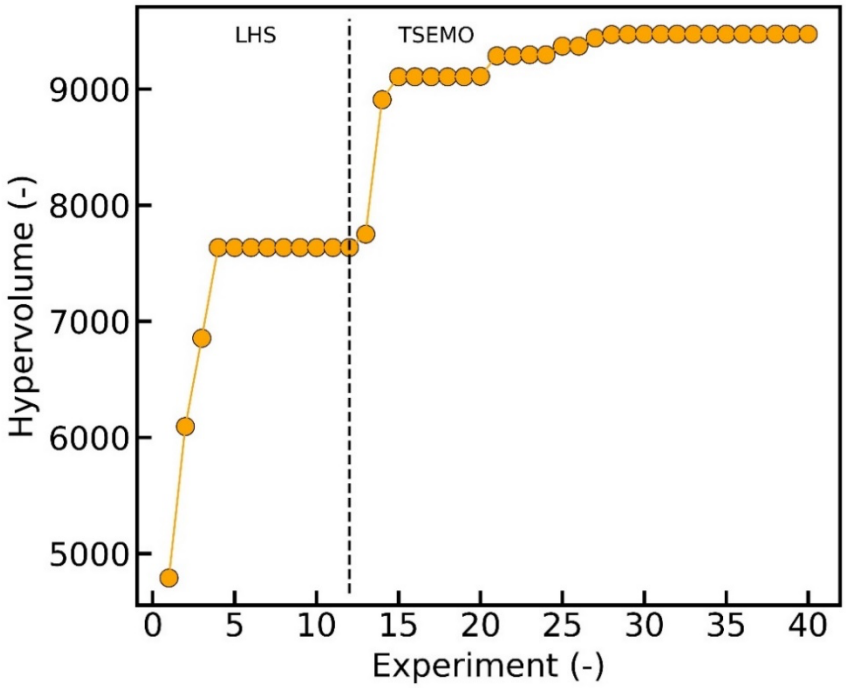

Figure S12.The change in the hypervolume during the course of optimization shown in **Figure 3.**

Table S4. Reaction conditions, yield, impurity and hypervolume values of optimization shown in **Figure 4.**

Experiment	τ (s)	T (°C)	nBuLi	Yield	Impurity	Hypervolume
Training-1	0.65	-28.33	1.225	67.85	29.42	4788.85
Training-2	0.989	-25.00	0.725	56.65	6.39	6093.50
Training-3	0.566	-21.67	1.058	75.28	16.73	6854.33
Training-4	0.396	-18.33	0.975	82.55	10	7634.01
Training-5	0.904	-15.00	1.308	56.65	35	7634.01
Training-6	0.819	-11.67	0.642	42.74	6.461	7634.01
Training-7	1.073	-8.33	0.808	56.5	6.9	7634.01
Training-8	1.158	-5.00	1.475	49	34.7	7634.01
Training-9	0.312	-1.67	1.558	40.67	51.23	7634.01
Training-10	0.227	1.67	1.392	65	28.35	7634.01
Training-11	0.735	5.00	1.142	41.95	28.43	7634.01
Training-12	0.481	8.33	0.892	42.84	16.3	7634.01
Optimization-1	0.654	-26.51	0.821	64.24	5	7750.70
Optimization-2	0.19	-23.43	1.063	93.94	5.57	8907.37
Optimization-3	0.189	-25.70	0.945	91.2	3	9105.14
Optimization-4	0.229	-17.20	1.066	88	8.9	9105.14
Optimization-5	0.185	-25.09	1.046	93.2	6	9105.14
Optimization-6	0.191	-30.00	1.167	83	16	9105.14
Optimization-7	0.185	-21.81	1.26	77.34	21.9	9105.14
Optimization-8	0.337	-25.88	1.013	93.7	4.45	9107.94
Optimization-9	0.24	-28.64	1.003	95.75	3.62	9284.93
Optimization-10	0.266	-23.49	1.005	95.68	3.26	9286.54
Optimization-11	0.194	-23.49	0.979	92.35	2.91	9295.15
Optimization-12	0.247	-23.52	1.019	93.41	4.38	9295.15
Optimization-13	0.41	-30.00	0.633	60	1.69	9368.35
Optimization-14	0.408	-23.76	0.938	84.5	5	9368.35
Optimization-15	0.197	-25.77	0.68	67	0.76	9439.20
Optimization-16	0.185	-24.08	0.868	84.2	1.16	9469.30
Optimization-17	0.243	-29.06	0.849	81.84	1	9471.68
Optimization-22	0.275	-27.36	0.861	85.5	2	9472.86
Optimization-18	0.185	-4.63	0.813	82	2.13	9472.86
Optimization-19	0.205	9.81	0.805	32	1.2	9472.86
Optimization-20	0.185	-10.54	0.786	70	2.1	9472.86
Optimization-21	0.322	-30.00	0.93	87	3.22	9472.86
Optimization-23	0.185	-3.20	0.608	57	1.85	9472.86
Optimization-24	1.2	-20.16	0.764	58	6.7	9472.86
Optimization-25	0.463	-29.95	0.893	85.42	1.99	9472.86
Optimization-26	0.437	-30.00	0.968	86	3.77	9472.86
Optimization-27	0.301	-25.09	0.791	73.6	1.65	9472.86
Optimization-28	0.388	-30.00	0.865	73.65	2.62	9472.86

8. Gaussian Process (GP) Regression Data

Table S5. Reaction conditions and experimental results to test the accuracy of the GP surrogate models built within TSEMO during optimization of Br-Li exchange reaction along with predictions and standard deviations of the predicted objectives from GP models. GP models built for the optimization campaign shown in Figure 2 were used to make predictions.

τ (s)	T (°C)	nBuLi	Yield	Impurity	Yield - GP	Yield - Std	Impurity - GP	Impurity - Std
0.27	-30	1.08	88	11	90.92	2.88	5.2	1.54
0.68	-29.01	1.6	34.8	34.7	27.19	16.09	43.45	9.2
0.28	-28.72	0.8	78.82	0.4	72.38	2.26	2.08	1.13
0.54	-28.33	1.17	47.3	19.47	61.83	8.36	13.94	5.55
0.65	-28	1.06	47.24	17.65	47.29	6.24	8.38	4.08
0.27	-27.71	1.24	85	14.9	77.25	8.13	22.5	6.45
0.97	-26.23	1	31.95	19.52	22.79	7	11.68	4.67
0.23	-21.76	1	92.55	4.28	90.44	1.78	4.39	0.83
0.9	-21.67	0.98	22.04	8.18	22.17	6.71	10.63	3.04
0.21	-20.8	1.22	80.57	19	82.71	6.42	19.98	4.98
0.32	-20.61	0.92	84.5	3.84	75.43	1.84	6.14	0.84
0.2	-19.72	0.81	75.97	0.96	78.29	1.73	0.78	0.78
0.99	-18.33	0.72	21.17	9.98	24.55	7.63	8.01	4.97
0.21	-15.08	0.84	69.86	1.55	78.05	2.09	3.39	1.07
1.16	-15	1.56	39.28	34.97	38.99	13.21	34.49	10.18
0.67	-13.87	0.99	34.4	14.39	43.8	6.22	15.06	2.79
0.26	-12.31	1.54	44	53	52.88	3.05	45.07	2.73
0.25	-12.24	0.6	57	1.5	53.34	4.93	4.33	3.68
0.31	-10.13	0.88	62.65	15.21	66.27	1.98	14.77	0.71
0.26	-8.33	0.97	77.5	8.95	77.45	3.6	17.48	2.76
0.31	-8	0.81	63.61	2.2	60.93	2.22	8.22	1.47
0.87	-5.57	0.98	29.88	28.4	25.04	6.93	22.49	4.61
1.07	-5	0.89	34.66	30.26	32.45	7.42	15.5	4.53
0.19	-4.26	1.15	90.82	7.59	81.17	3.85	17.76	1.68
0.21	-3.69	0.9	71.43	1.97	75.89	5.01	14.23	3.25
0.4	-1.67	0.83	68.76	4.43	53.33	3.21	13.6	2.68
0.38	2.72	1	64.93	14.3	67.02	6.76	24.17	5.8
0.47	5	1.23	63.97	27.97	64.44	6.8	26.15	3.64
0.57	5	1.14	62.96	20.99	59.01	7.76	33.79	5.27
0.37	8.61	0.8	72.5	8.4	53.28	4.36	5.89	1.92

SI References

[1] O. Levenspiel, *Chemical reaction engineering*. John Wiley & Sons, 1998.

[2] W. Schotte, Prediction of the molar volume at the normal boiling point, *The Chemical Engineering Journal,* 48:3, 167-172, 1992.

[3] http://www.ddbst.com/en/EED/PCP/VIS_C159.php